Peptide Binding and NMR Analysis of the Interaction between SAP97 PDZ2 and GluR-A: Potential Involvement of a Disulfide Bond†

Lotta von Ossowski,‡ Helena Tossavainen,§ Ingemar von Ossowski,‡ Chunlin Cai,‡ Olli Aitio,|| Kai Fredriksson,§ Perttu Permi,§ Arto Annila,‡,§ and Kari Keinänen*,‡

Department of Biological and Environmental Sciences (Division of Biochemistry), Program in Structural Biology and Biophysics, Institute of Biotechnology, and Drug Discovery and Development Technology Center, Faculty of Pharmacy, University of Helsinki, Helsinki, Finland

Received June 22, 2005; Revised Manuscript Received March 10, 2006

ABSTRACT: Synaptic delivery of GluR-A (GluR1) subunit-containing glutamate receptors depends on a C-terminal type I PDZ binding motif in GluR-A. Synapse-associated protein 97 (SAP97) is the only PDZ domain protein known to associate with GluR-A. We have used NMR spectroscopy and a biotinylated peptide binding assay to characterize the interaction between synthetic GluR-A C-terminal peptides and the PDZ2 domain of SAP97 ($SAP97_{PDZ2}$), previously determined to be the dominant factor responsible for the interaction. The binding mode appeared to be strongly influenced by redox conditions. Chemical shift changes observed in NMR spectra indicate that under reducing conditions, the last four residues of GluR-A peptides bind to PDZ2 in a fashion typical of class I PDZ interactions. The binding is weak and relatively nonselective as it occurs similarly with a PDZ2 domain derived from PSD-95, a related protein not believed to directly interact with GluR-A. In the absence of reducing agents, conserved cysteine residues in $SAP97_{PDZ2}$ and the GluR-A C-terminus gave rise to an anomalous behavior in a microplate assay with a biotinylated GluR-A 18-mer peptide. A covalent disulfide-linked complex between $SAP97_{PDZ2}$ and the GluR-A peptide was seen in the binding assay and in the NMR experiments performed under oxidizing conditions. The results are consistent with a two-step binding mechanism consisting of an initial PDZ interaction followed by stabilization of the complex by a disulfide bond. The possible physiological relevance of redox regulation of SAP97−GluR-A interaction remains to be established.

Synapse-associated protein 97 (SAP97)[1] and its close relatives SAP102, postsynaptic density-95 (PSD-95), and PSD-93 form a family of membrane-associated guanylate kinase homologues (Maguks), the members of which are believed to function as molecular scaffolds in cellular trafficking, anchoring to cytoskeleton, and assembly of signaling machineries of synaptic receptors and channels (*1*). Consistent with such a scaffolding role, these proteins harbor multiple protein interaction domains, including three PDZ domains, an SH3 domain, and a catalytically inactive guanylate kinase domain (*1*).

Transport of AMPA-type glutamate receptors to and from synapses, a process guided by the cytoplasmic C-terminal tails of receptor subunits, is assumed to be one of the key mechanisms in the regulation of synaptic strength (*2*, *3*). Activity-dependent insertion of new AMPA receptors into synapses critically depends on the presence of a class I PDZ binding motif [-x-S/T-x-ϕ, where S is serine, T is threonine, ϕ is a hydrophobic amino acid, and x is any amino acid (*4*)] at the carboxyl terminus of AMPA receptor subunit GluR-A (GluR1) (*5*). GluR-A has been reported to associate, via C-terminal interactions, with SAP97 (*6*), 4.1N (*7*), RIL (*8*), and mLin-10 (*9*), all multidomain proteins potentially involved in GluR-A transport. To date, however, the interaction between SAP97 and GluR-A is the only one for which a strict dependency on the class I PDZ binding motif has been observed (*6*, *10*). Accordingly, the role of this interaction in AMPA receptor trafficking has come under intense scrutiny (*11*−*13*).

Previously, we have shown that the C-terminal domain (CTD) of GluR-A binds to the PDZ domains of SAP97 but not to those of PSD-95, PSD-93, and SAP102 and that the second PDZ domain ($SAP97_{PDZ2}$) forms the predominant binding site in glutathione *S*-transferase (GST) pulldown assays (*10*). Such a selectivity is unusual because of the

† This work was supported by The National Graduate School in Informational and Structural Biology (L.v.O.) and the Academy of Finland (202892 and 205778).

* To whom correspondence should be addressed: Department of Biological and Environmental Sciences, Division of Biochemistry, P.O. Box 56 (Viikinkaari 5), University of Helsinki, FI-00014 Helsinki, Finland. Telephone: +358-9-19159606. Fax: +358-9-19159068. E-mail: kari.keinanen@helsinki.fi.

‡ Department of Biological and Environmental Sciences (Division of Biochemistry).

§ Program in Structural Biology and Biophysics, Institute of Biotechnology.

|| Drug Discovery and Development Technology Center, Faculty of Pharmacy.

[1] Abbreviations: AMPA, α-amino-3-hydroxy-5-methyl-4-isoxazolepropionic acid; BSA, bovine serum albumin; CTD, carboxy-terminal domain; GluR-A, ionotropic glutamate receptor subunit A; nOe, nuclear Overhauser enhancement; NTD, amino-terminal domain; PDZ, postsynaptic density −95/discs large/zona occludens-1; PSD-93, postsynaptic density 93; PSD-95, postsynaptic density 95; SAP97, synapse-associated protein 97; SAP102, synapse-associated protein 102; SDS−PAGE, sodium dodecyl sulfate−polyacrylamide gel electrophoresis.

10.1021/bi0511989 CCC: $33.50
Published on Web 04/08/2006

~90% degree of identity between the amino acid sequences of the respective PDZ2 domains. To further characterize the structural basis of GluR-A−SAP97 interaction, we have studied the binding of synthetic C-terminal peptides to $SAP97_{PDZ2}$ and identified the key structural determinants by NMR spectroscopy. We found that redox conditions strongly affect the binding mode. Under reducing conditions, a conventional class I PDZ interaction is observed, whereas in the absence of a reducing agent, formation of an intermolecular disulfide between a GluR-A C-terminal peptide and $SAP97_{PDZ2}$ dominates the interaction. Our results suggest a possibility that the interaction between SAP97 and GluR-A is under redox regulation.

MATERIALS AND METHODS

Plasmid Construction. A DNA fragment encoding the second PDZ segment (residues 315−409) of rat SAP97 was produced by PCR from the full-length template with the primers 5′-GTTGGTCCATGGAAAAAATCATGGAAATA-AAACT-3′ (sense) and 5′-GGTGTTTCTAGATATATA-CATACTTGTTGGTT-3′ (antisense). The DNA sequence encoding rat $PSD\text{-}95_{PDZ2}$ (residues 156−252) was similarly amplified by using primers 5′-GTTGGTCCATGGAAAAG-GTCATGGAGATCAAACT-3′ (sense) and 5′-GGTGTT-TCTAGACAGGTAGGCATTGCTGGGCTA-3′ (antisense). DNA encoding the N-terminal domain of SAP97 ($SAP97_{NTD}$) was amplified with primers 5′-GGTGTTCCATGGCCAT-GCCGGTCCGGAAGCAAGAT-3′ (sense) and 5′-GGT-GTTTCTAGACTCATATTCATAATCTGCATC-3′ (anti-sense). Gel-purified PCR fragments were digested with NcoI and XbaI (restriction sites underlined in the primer sequences) and ligated into a similarly treated T7 expression plasmid which harbors a sequence encoding a six-His tag positioned after the XbaI site (*10*). A cysteine-to-serine (C378S) mutant of $SAP97_{PDZ2}$ was generated by PCR and cloned into the T7 expression vector. The final constructs were fully sequenced and transformed in *Escherichia coli* BL21(DE3)pLysS for expression. The predicted amino acid sequence of the recombinant $SAP97_{PDZ2}$ construct (105 residues, theoretical molecular mass of 11 450.2 Da) starts with MEKIMEIKLIK and ends with KPTSMYSRHHH-HHH. The predicted sequence of $PSD\text{-}95_{PDZ2}$ (105 residues, theoretical molecular mass of 11 371.0 Da) starts with MEKVMEIKLIK and ends with PSNAYLSRHHHHHH, whereas $SAP97_{NTD}$, produced as a control protein for peptide binding studies, has 200 residues (theoretical molecular mass of 22 609.0 Da) with the following predicted amino acid sequence: MAMPVRKQDTQ...DYEYESRHHHHHH.

Expression and Purification of His-Tagged Proteins for the Binding Assay. $SAP97_{PDZ2}$, $PSD\text{-}95_{PDZ2}$, $SAP97_{PDZ2}$ C378S, and $SAP97_{NTD}$ were expressed in *E. coli* BL21(DE3)-pLysS using LB medium for growth and standard procedures for induction (*pET System Manual*, 10th ed., Novagen Corp., 2002). Soluble protein was released from bacterial pellets by sonication in lysis buffer [50 mM NaH_2PO_4, 300 mM NaCl, and 10 mM imidazole (pH 7.4)], whereafter His-tagged PDZ domains were purified by immobilized metal chelation affinity chromatography on a Ni^{2+}−NTA matrix. Bound protein was eluted in elution buffer containing 250 mM imidazole. The elution buffer was exchanged with 10 mM Bis-Tris by passing the purified protein over an Econo-Pac 10DG gel filtration column (Bio-Rad, Espoo, Finland).

SDS−PAGE. Protein preparations were resolved by electrophoresis using precast linear 18% or 4 to 20% gradient gels (Bio-Rad) and stained with Coomassie Brilliant Blue R250. Prior to electrophoresis, samples were heated for 5 min at 95 °C in the presence or absence of β-mercaptoethanol. Rat brain GluR-A and SAP97 were solubilized as described previously (*10*) and resolved by SDS−PAGE (7.5% gel) with or without prior treatment with β-mercaptoethanol, transferred to a polyvinylidene difluoride filter, and subjected to immunoblotting with SAP97 and GluR-A-specific antibodies.

Peptide Binding Assay. Microtiter plates (96-well, Greiner Bio-One, Frickenhausen, Germany) were coated with purified $SAP97_{PDZ2}$ or control proteins (all at 5 μg/mL in PBS) overnight at 4 °C. After the nonspecific protein binding had been blocked (1% BSA in PBS, 3 h at room temperature), N-terminally biotinylated GluR-A C-terminal 18-mer peptide (residues 890−907, $Bio\text{-}GluRA_{18}$) was added to a final concentration of 0.3−30 μM for a 60−120 min incubation at room temperature. The wells were washed briefly with 0.05% Tween 20 in PBS and incubated with alkaline phosphatase-conjugated streptavidin (Jackson ImmunoResearch Laboratories, Cambridgeshire, U.K.) for 60 min. Finally, 13.5 mM 4-nitrophenyl phosphate in 1 M diethanolamine (pH 9.8) and 0.5 mM $MgCl_2$ was added as a colorigenic substrate. Absorbance values at 405 nm were measured by using a Multiskan EX plate reader (Thermo Labsystems, Vantaa, Finland). For the validation of the assay and for control purposes, the N-terminally biotinylated 14-mer C-terminal peptide of NMDA receptor subunit NR2A (residues 1451−1464, $Bio\text{-}NR2A_{14}$) was used as the ligand instead of $Bio\text{-}GluRA_{18}$. All synthetic peptides used in this study were obtained from Sigma-Genosys (Haverhill, U.K.) and were >95% pure.

Mass Spectrometry Analysis. MALDI-TOF mass spectrometry of $SAP97_{PDZ2}$ and tryptic digests thereof was performed on an Ultraflex TOF/TOF instrument (Bruker Daltonik, Bremen, Germany) in the Protein Chemistry Unit of the Institute of Biotechnology, University of Helsinki. Expected masses of trypsin-cleaved SAP97 fragments were calculated using PeptideMass Peptide Characterization Software (*14*) for comparison to the experimental values.

Preparation of Isotope-Labeled Samples for NMR Spectroscopy. For isotope labeling of $SAP97_{PDZ2}$, LB medium was replaced with M9 minimal medium supplemented with [^{13}C]glucose (2 g/L) and [^{15}N]ammonium chloride (1 g/L) as the sources of carbon and nitrogen. The PDZ domain was purified as described above. For NMR spectroscopy, ^{13}C- and ^{15}N-labeled $SAP97_{PDZ2}$ was prepared as a 1 mM solution in Bis-Tris (pH 6.5) in a Shigemi 250 μL microcell. Nonlabeled $SAP97_{PDZ2}$ and $PSD\text{-}95_{PDZ2}$ were prepared to comparable concentrations.

NMR Spectroscopy and Chemical Shift Assignment. Multidimensional heteronuclear correlation spectra were acquired at 25 °C from $SAP97_{PDZ2}$ to assign main chain, C^{β} (*15*, *16*), and methyl resonances (*17*) using Varian Unity Inova 600 and 800 MHz spectrometers, equipped with actively shielded *z*- and *xyz*-axis gradient triple-resonance probeheads. The spectra were processed with Vnmr (Varian Inc., Palo Alto, CA) and analyzed with Sparky version 3.106 (Goddard, T. D., and Kneller, D. G. *Sparky*, version 3.106, University of California, San Francisco). The backbone resonances were

initially assigned using Autoassign (*18*) and finalized manually. The assignment was complete for the backbone, excluding the N-terminal amide group, and for all C^{β} and methyl groups. The methyl groups were assigned using the DE-MQ-(H)CC_mH_m-TOCSY experiment (*17*) to correlate the C^{α} and C^{β} chemical shifts with those of methyl carbons and protons. $GluRA_{13}$ and $GluRA_{18}$ peptides were assigned completely from two-dimensional homonuclear correlation spectra (*19*).

To analyze complex formation, the $SAP97_{PDZ2}$ and $PSD\text{-}95_{PDZ2}$ solutions were titrated separately to $GluRA_{13}$ peptide solutions up to 1:1 molar ratios while the peptide aliphatic resonances were monitored to identify GluR-A binding structures. When titration was carried out with $SAP97_{PDZ2}$, the peptide contained a reducing agent (10 mM DTT) to prevent disulfide-mediated dimerization of the PDZ domain. In a complementary fashion, the binding epitopes in $SAP97_{PDZ2}$ were assessed by monitoring the amide shift changes from $^{15}N-^{1}H$ correlation spectra while the $GluRA_{13}$ peptide was titrated to a 10-fold molar excess. We computed (*20*) an overall figure of merit $\{\Delta\delta_{av} = {}^{1}/_{4}\sqrt{[(\Delta\delta_{HN})^2 + (\Delta\delta_N/5)^2 + (\Delta\delta_{C^{\alpha}}/2)^2 + (\Delta\delta_{C^{\beta}}/2)^2]}\}$ of secondary shifts per residue and considered the following significant: $\Delta\delta_{HN} > 0.03$, $\Delta\delta_N > 0.3$, $\Delta\delta_{C^{\alpha}} > 0.3$, and $\Delta\delta_{C^{\beta}} > 0.3$ ppm. A series of two-dimensional NOE spectra with increasing mixing times from 100 to 600 ms were recorded for the $GluRA_{13}/SAP97_{PDZ2}$ (10:1) sample. Furthermore, the binding of $GluRA_{18}$ was analyzed in the absence of a reducing agent because the plate binding assays indicated formation of a disulfide bond between the peptide and $SAP97_{PDZ2}$. Finally, the $SAP97_{PDZ2}$ sample was purified from the excess of $GluRA_{18}$ by centrifugal ultrafiltration and dialysis using Vivaspin concentrators (Vivascience, Hannover, Germany) with a 5K cutoff, and the $^{15}N-^{1}H$ correlation spectrum of $SAP97_{PDZ2}$ in a covalent complex with GluR-A was acquired to assess the occupancy of the PDZ binding site in the presence of disulfide.

Model Building. For the initial model of the complex, the PDZ2 homology model was kept fixed and the conformation of the GluR-A peptide was searched by annealing. On the basis of chemical shift perturbations, it is unknown a priori which groups of the receptor and ligand are adjacent to each other. Therefore, initially all secondary chemical shifts were mapped to a set of ambiguous distance restraints. Because of the $1/r^6$ averaging, any incorrect restraint among the sum of restraints will acquire only a very small weight, and thus, its influence will be negligible provided that the ambiguous restraint set contains at least one correct restraint (*21*). During the latter part of the simulated annealing protocol, side chains of the PDZ model were allowed to move to accommodate the peptide ligand. The side chain rotamers were refined according to conformational database potential (*22*). The main chain dihedrals of the C-terminus of GluR-A were restrained to the β-conformation on the basis of the strong intramolecular NOEs recorded from the complex and Hα chemical shifts that experienced a downfield shift upon binding, i.e., toward β-sheet values. An initial model of the bound peptide conformation allowed us to rationalize the spectral changes as those caused primarily by filling the binding groove and those due to the secondary effects. We refined our model by excluding those restraints that corresponded to secondary effects far from the binding site.

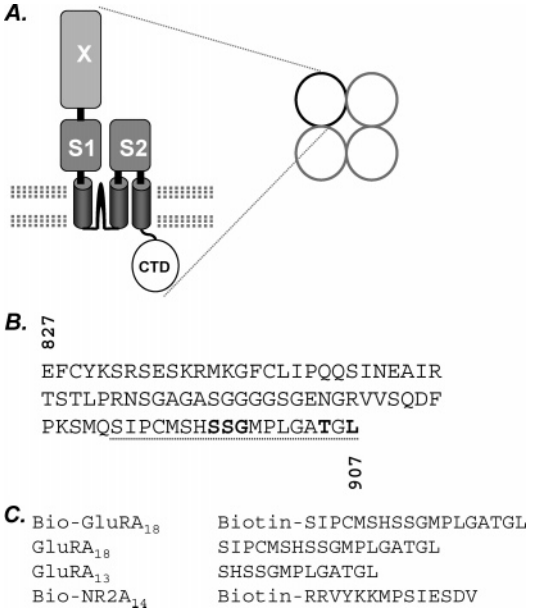

FIGURE 1: Schematic structure of GluR-A. (A) Domain organization of tetrameric AMPA receptors. The membrane topology of a single GluR-A subunit is shown: X, N-terminal domain; S1 and S2, two-lobed ligand binding domain; CTD, cytoplasmic carboxy-terminal domain. (B) Amino acid sequence of GluR-A CTD. The residues found to be essential for the interaction with SAP97 PDZ domains in GST pulldown assays are in bold type. (C) Synthetic peptides used in this study.

In the initial model, the C-terminal leucine residue (Leu907, position 0 in the $GluRA_{13}$ peptide) was localized to attribute its secondary shifts to the GLGF motif and vice versa. In the refined model, characteristic class I PDZ interactions became apparent. The backbone amide shift changes of GLGF motif were attributed to a neutralizing interaction with the terminal carboxylate of Leu907. The large aliphatic shifts of the threonine (Thr905) and alanine (Ala904) residues at positions −2 and −3 of $GluRA_{13}$, respectively, were associated with the side chain of His384 of $SAP97_{PDZ2}$ because the shift perturbation of the methyl group of Thr905 supported the presence of a hydrogen bond between the hydroxyl of Thr905 and the ring nitrogen of His384. This was modeled as a restraint in the final calculation.

RESULTS

Earlier GST pulldown experiments indicated that a class I PDZ motif at the GluR-A C-terminus, together with an upstream tripeptide sequence SSG, is essential for binding of GluR-A CTD to SAP97 PDZ domains (*9*) (Figure 1A,B). In this study, we employed NMR spectrocopy to analyze the structural basis of the interaction. Our efforts to produce the GluR-A CTD (residues 827−907) as a soluble polypeptide at concentrations sufficient for detailed analyses were not successful, and therefore, synthetic GluR-A C-terminal peptides were chosen as surrogates for the cytoplasmic domain (Figure 1C).

C-Terminally His-tagged $SAP97_{PDZ2}$ and $PSD\text{-}95_{PDZ2}$ were expressed in *E. coli* and purified by using immobilized metal chelation affinity chromatography. In SDS−PAGE analysis, the purified $SAP97_{PDZ2}$ preparations contained a major 12 kDa band. In gels loaded with larger amounts of protein, the presence of an additional 24 kDa species became

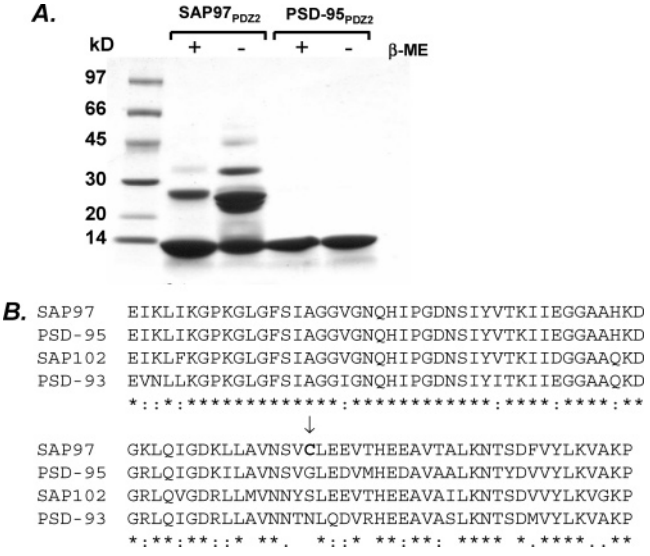

FIGURE 2: Disulfide-dependent dimerization of $SAP97_{PDZ2}$. (A) SDS−polyacrylamide gel electrophoresis of purified $SAP97_{PDZ2}$ and $PSD\text{-}95_{PDZ2}$ preparations analyzed with or without prior reduction using 2-mercaptoethanol (β-ME). (B) Sequence alignment (CLUSTAL W 1.82) of the second PDZ domains of rat PSD-95 family Maguk proteins. The single cysteine residue present in SAP97 (Cys378) is denoted with an arrow.

apparent, in particular with samples stored at 4 °C for several days (Figure 2A). Under nonreducing conditions, the 24 kDa band was often more pronounced, and additional faint bands of ~35 and ~50 kDa became visible. The 24 kDa species may represent a dimer stabilized by a disulfide bond as the PDZ2 domain of SAP97 contains a single conserved cysteine (C378), not present in the PDZ2 domains of related PSD-95, PSD-93, and SAP102 (Figure 2B). Consistent with this, $PSD\text{-}95_{PDZ2}$ expressed in parallel migrated as a major 12 kDa species under both reducing and nonreducing conditions (Figure 2A). In immunoblotting, both the 12 and 24 kDa bands were recognized by the anti-His antibody (results not shown). Mass spectrometric analysis of tryptic peptides provided further evidence for the identity of the 24 kDa band as a PDZ dimer. Three major tryptic mass peaks produced by the reduced and alkylated 12 and 24 kDa bands were 2501.280 and 2501.284 (theoretical, 2501.2782; peptide, GLGFSIAGGVGNQHIPGDNSIYVTK), 2425.240 and 2425.250 (2425.2642; LLAVNSVCLEEVTHEEAVTALK), and 1252.675 and 1252.674 (1252.6718; VAKPTSMYISR). The origin of the ~35 and ~50 kDa species has not been determined, but they are likely to represent non-disulfide-bonded but SDS-resistant aggregates of the 24 kDa PDZ2 dimer with a monomeric PDZ2 and with another dimer, respectively.

To characterize the interaction of GluR-A C-terminal peptides with $SAP97_{PDZ2}$, we first employed a plate assay. The binding of the N-terminally biotinylated 18-mer GluR-A pepide ($Bio\text{-}GluRA_{18}$) to microtiter wells coated with purified $SAP97_{PDZ2}$ was assessed by using a streptavidin−alkaline phosphatase conjugate and colorigenic substrate. An 18-mer GluR-A peptide was chosen for the binding studies because of our earlier finding of the importance of sequences upstream from the C-terminal PDZ motif (*10*) and to provide sufficient distance between the N-terminally conjugated biotin and the assumed binding determinants in the plate binding assay. As a positive control, we used a biotinylated 14-mer C-terminal peptide ($Bio\text{-}NR2A_{14}$) derived from the NR2A subunit of the NMDA receptor, which binds to the first two PDZ domains of PSD-95 family Maguks with micromolar affinity (*23*−*25*). As negative controls, wells were coated with the N-terminal domain of SAP97 ($SAP97_{NTD}$) or with BSA. $Bio\text{-}NR2A_{14}$ bound to immobilized $SAP97_{PDZ2}$ in a saturable manner with an apparent affinity of 0.40 ± 0.05 μM (mean ± standard error of the mean of three replicate values) but did not exhibit any significant binding to the N-terminal domain of SAP97 (Figure 3A). Binding of the $Bio\text{-}GluRA_{18}$ peptide $SAP97_{PDZ2}$ appeared saturable with an apparent affinity of 5.98 ± 1.20 μM. $Bio\text{-}GluRA_{18}$ bound weakly to immobilized $SAP97_{NTD}$, and the extent of binding was linearly dependent on the peptide concentration (Figure 3A). Neither peptide exhibited any significant binding to BSA-coated wells (results not shown). In the presence of a 40-fold molar excess of unlabeled $GluR\text{-}A_{18}$ and $NR2A_{14}$ peptides, binding of the respective biotinylated peptides was strongly inhibited (Figure 3B). Surprisingly, however, the $GluRA_{18}$ peptide inhibited the binding of $Bio\text{-}NR2A_{14}$ only relatively weakly, whereas the $NR2A_{14}$ peptide did not cause any significant inhibition of $Bio\text{-}GluRA_{18}$ binding (Figure 3B).

We suspected that the cysteine residues present in the $GluRA_{18}$ peptide and $SAP97_{PDZ2}$ may be the cause for the anomalous binding of $Bio\text{-}GluRA_{18}$, and therefore, we tested the effects of thiol regents on peptide binding. Dithiothreitol (10 mM) strongly inhibited binding of $Bio\text{-}GluRA_{18}$ but had an only minor effect on $Bio\text{-}NR2A_{14}$ binding. The binding results suggest that $Bio\text{-}GluR\text{-}A_{18}$ binds to $SAP97_{PDZ2}$ with an intrinsic low affinity, but under nonreducing conditions, it is able to form an intermolecular disulfide bond with the PDZ domain, leading to a covalent complex. Considering the tendency of $SAP97_{PDZ2}$ to form disulfide-bonded dimers, an alternative explanation for the findings described above is that the GluR-A peptide may bind only to a disulfide-linked PDZ dimer. To distinguish between these possibilities, $SAP97_{PDZ2}$-coated wells were subjected to 10 mM dithiothreitol or *N*-ethylmaleimide (60 min, room temperature), followed by incubation with $Bio\text{-}GluRA_{18}$ in the presence or absence of these thiol reagents. Both reagents caused a complete block of $Bio\text{-}GluRA_{18}$ binding when present throughout the assay. Interestingly, however, dithiothreitol pretreatment significantly enhanced whereas *N*-ethylmaleimide largely blocked the subsequent $Bio\text{-}GluRA_{18}$ binding under nonreducing conditions (Figure 3C). These findings indicate that $Bio\text{-}GluRA_{18}$ forms a disulfide bond with $SAP97_{PDZ2}$. The enhanced binding induced by prior exposure to dithiothreitol is likely to be caused by conversion of disulfide-linked PDZ domains to a reduced state, whereas inhibition by *N*-ethylmaleimide is consistent with inactivation of cysteine thiols through alkylation. Indeed, electrophoretic analysis of a 1:1 mixture of $Bio\text{-}GluRA_{18}$ and $SAP97_{PDZ2}$ by alkaline phosphatase-conjugated streptavidin blotting revealed the presence of an intermolecular SDS-resistant complex which was eliminated by reduction prior to electrophoresis (Figure 3D). To further confirm the disulfide complex between the peptide and the PDZ domain, Cys378 was replaced with a serine residue. In the plate binding assay, wells coated with $SAP97_{PDZ2}$ C378S did not bind $Bio\text{-}GluRA_{18}$ above the background obtained with BSA coating

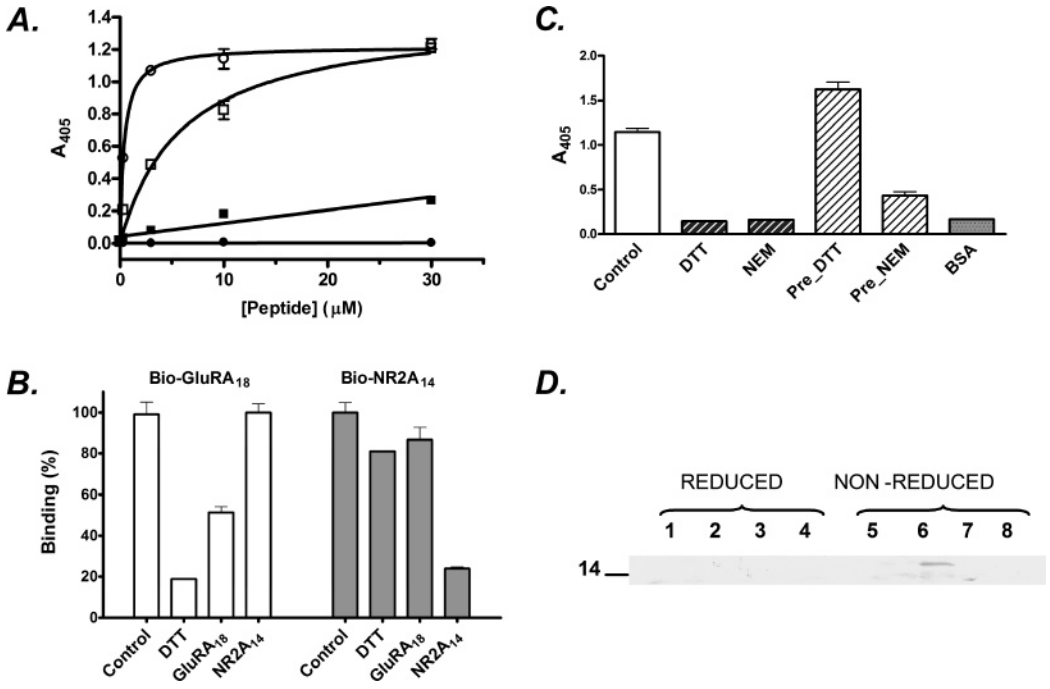

FIGURE 3: Binding of biotinylated peptides to $SAP97_{PDZ2}$. (A) Binding of Bio-$GluRA_{18}$ (squares) and Bio-$NR2A_{14}$ (circles) to immobilized $SAP97_{PDZ2}$ (empty symbols) and $SAP97_{NTD}$ (filled symbols). Nonlinear curve fitting of specific binding yields apparent affinities of 5.98 and 0.40 μM for Bio-GluR-A_{18} and Bio-$NR2A_{14}$, respectively. (B) Effect of 10 mM dithiothreitol and unlabeled GluR-A_{18} or $NR2A_{14}$ peptides (each at 200 μM) on the binding of Bio-$GluRA_{18}$ and Bio-$NR2A_{14}$ (both at 10 μM) to $SAP97_{PDZ2}$. Binding is normalized with respect to the A_{405} values (mean ± standard error of the mean of triplicate samples) obtained in the absence of unlabeled peptides or DTT (equivalent to 100%). (C) Effect of thiol reagents on the binding of Bio-GluR-A_{18} to $SAP97_{PDZ2}$. $SAP97_{PDZ2}$-coated wells were exposed to dithiothreitol (10 mM) or *N*-ethylmaleimide (10 mM) for 1 h, whereafter the binding of Bio-GluR-A_{18} was assessed in the presence (DTT, NEM) or absence (Pre_DTT, Pre_NEM) of the reagents. Binding of Bio-GluR-A_{18} to $SAP97_{PDZ2}$ (Control) and to bovine serum albumin (BSA) in the absence of DTT and NEM is shown as well. (D) Covalent coupling of Bio-GluR-A_{18} to $SAP97_{PDZ2}$. $SAP97_{PDZ2}$ (lanes 1, 2, 5, and 6) or $SAP97_{PDZ2}$ C378S (lanes 3, 4, 7, and 8) was incubated at 8 μM either alone (lanes 1, 3, 5, and 7) or together with 8 μM Bio-GluR-A_{18} (lanes 2, 4, 6, and 8) for 24 h at room temperature followed by SDS−PAGE under reducing or nonreducing conditions as indicated. Biotin was visualized on nitrocellulose blot transfers by using streptavidin-conjugated alkaline phosphatase.

(result not shown), nor did it form a covalent complex with the peptide (Figure 3D).

To obtain information about the possible in vivo significance of a disulfide linkage between GluR-A and SAP97, rat brain detergent extracts were analyzed. Analysis of immunoprecipitates under nonreducing conditions was not successful largely due to an intense high-molecular weight background produced by immunoglobulins. In direct immunoblots, however, interesting differences in the electrophoretic mobilities of SAP97 and GluR-A were observed between reduced and nonreduced samples. GluR-A, which appeared as an ~100 kDa band under reducing conditions, migrated almost entirely as >250 kDa diffuse species (Figure 1 of the Supporting Information). Additional immunoreactive bands in the high-molecular weight region, partly overlapping with GluR-A bands, were observed for nonreduced SAP97 as well (Figure 1 of the Supporting Information). These findings suggest that the native GluR-A and SAP97 are involved in disulfide-linked complexes in vivo, although their molecular identity and nature are unclear at present.

Next, NMR spectroscopy was used to obtain structural information about the interaction of GluR-A peptides with SAP97. For NMR studies, SAP97 preparations with little dimer or no dimers visible in SDS−PAGE were used. In addition, 10 mM DTT was included to prevent formation of PDZ dimers during the experiments. From the overall amide signal dispersion of $SAP97_{PDZ2}$, which was comparable to the corresponding $PSD\text{-}95_{PDZ2}$ spectrum (*26*), we inferred that $SAP97_{PDZ2}$ is well-folded. Furthermore, the backbone chemical shift index indicated that the overall fold is similar to that of PSD-95, consistent with the high level of sequence identity. Because none of the nine sequence differences between the PDZ2 domains of PSD-95 and SAP97 are in the peptide binding pocket that includes the conserved GLGF motif of the βA−βB loop and the His residue at αB, we reasoned that the PSD-95 PDZ2 solution structure [PDB entry 1QLC (*26*)] can be used as homology model for $SAP97_{PDZ2}$ to interpret the NMR data.

Subsequently, binding of a 13-mer GluR-A peptide, $GluRA_{13}$, was analyzed. Upon peptide titration, we observed a number of $SAP97_{PDZ2}$ chemical shift changes with no differences observed between $GluRA_{13}$ and $GluRA_{18}$. As expected, the PDZ binding pocket was the locus of the largest shift perturbations (Figure 4A). In addition to the primary effects, minor shift changes were found adjacent to the binding groove. These may arise from minor structural rearrangements in the whole PDZ2 domain when the binding site becomes occupied. In general, the observed secondary shifts are comparable to those observed when PSD-95 PDZ2 makes a complex with the β-finger peptide of the nNOS PDZ2 domain (*27*). Of the nine sequence differences between the PDZ2 domains of SAP97 and PSD-95, significant chemical shift perturbations were observed at three residues, Leu371 (corresponding to Ile212 of PSD-95), Thr383 (Met224), and Thr389 (Ala230). The chemical shifts of the latter two residues were observed to change in the PSD-

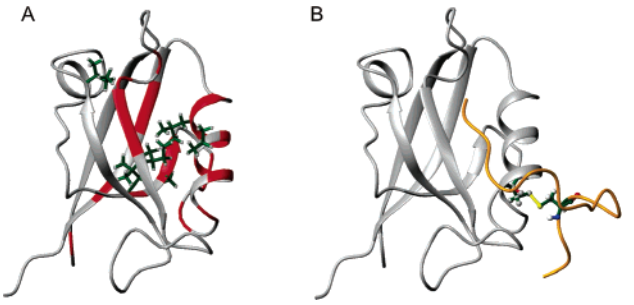

FIGURE 4: Average chemical shift perturbations ($\Delta\delta_{av}$) of $SAP97_{PDZ2}$ induced by formation of the complex with GluR-A. $\Delta\delta_{av}$ values of ≥ 0.05 ppm (^1H, ^{15}N, $^{13}C\alpha$, and $^{13}C\beta$) are colored red. The side chains of the residues whose methyl groups were perturbed are also shown. (B) Representative backbone model of the $GluRA_{18}$ peptide in complex with a homology model of $SAP97_{PDZ2}$ built on the basis of chemical shift perturbation and nuclear Overhauser enhancements. The cysteines in the disulfide are shown specifically.

Table 1: Chemical Shift Changes Observed in $GluRA_{13}$ Titrated with $SAP97_{PDZ2}$

residue	atom	$\delta\Delta^a$ (Hz)	residue	atom	$\delta\Delta^a$ (Hz)
Leu13	H^{α}	8.8	Pro7	H^{α}	1.6
	$H^{\beta 2/\beta 3/\gamma}$	−13.6		$H^{\beta 2/\beta 3}$	6.4/0.0
	$H^{\delta 1/\delta 2}$	−35.2/−12.8		$H^{\gamma 2/\gamma 3}$	7.2
Gly12	$H^{\alpha 2/\alpha 3}$	overlap		$H^{\delta 2/\delta 3}$	1.6/4.0
Thr11	H^{α}	6.4	Met6	H^{α}	0.8
	H^{β}	−33.6		$H^{\beta 2/\beta 3}$	6.4/2.4
	$H^{\gamma 2}$	4.0		$H^{\gamma 2/\gamma 3}$	4.8/−0.8
Ala10	H^{α}	53.6	Gly5	$H^{\alpha 2/\alpha 3}$	overlap
	H^{β}	−13.6	Ser4/3	H^{α}	1.6/−0.8
Gly9	$H^{\alpha 2/\alpha 3}$	overlap		$H^{\beta 2/\beta 3}$	−0.8/1.6/0.0/0.0
Leu8	H^{α}	0.8	His2	H^{α}	0.0
	$H^{\beta 2/\beta 3}$	5.6		$H^{\beta 2/\beta 3}$	1.6/−0.8
	H^{γ}	0.8		$H^{\delta 2/\epsilon 1}$	−0.8/−1.6
	$H^{\delta 1/\delta 2}$	4.0/3.2	Ser1		not visible

[a] At a 0.6:1 protein:peptide ratio.

95−nNOS PDZ2 complex as well (*27*). Ile212 is located in the core of the PSD-95 structure. Its chemical shift change most probably arises from the domain's structural rearrangement upon binding since the shortest distance between the residue and the peptide in our model (see below) is more than 8 Å.

In complementary experiments, $SAP97_{PDZ2}$ and $PSD\text{-}95_{PDZ2}$ were titrated in a $GluRA_{13}$ peptide solution. The observed secondary aliphatic shifts were noticed exclusively at the very last C-terminal residues (Table 1), being spatially complementary to signal changes in PDZ2 and implying an extended C-terminus for $GluRA_{13}$. No significant differences in $GluRA_{13}$ secondary chemical shifts were observed between $SAP97_{PDZ2}$ and $PSD\text{-}95_{PDZ2}$ titrations. Thus, we conclude that the C-terminal ATGL motif accounts for the binding of the GluR-A peptide under reducing conditions.

We built a structural model of the complex on the basis of the observed secondary chemical shifts and intramolecular nOes (see Table 1 of the Supporting Information). We were unable to identify any intermolecular nOes. Our objective in model building was to test the disulfide bonding hypothesis rather than to obtain a very precise model. The model building protocol (for details, see Materials and Methods) was similar to that employed in constructing a protein complex by a rigid body minimization where spectral changes are interpreted as proximal effects (*28*). Consequently, the precision of our model of $GluRA_{13}$ when

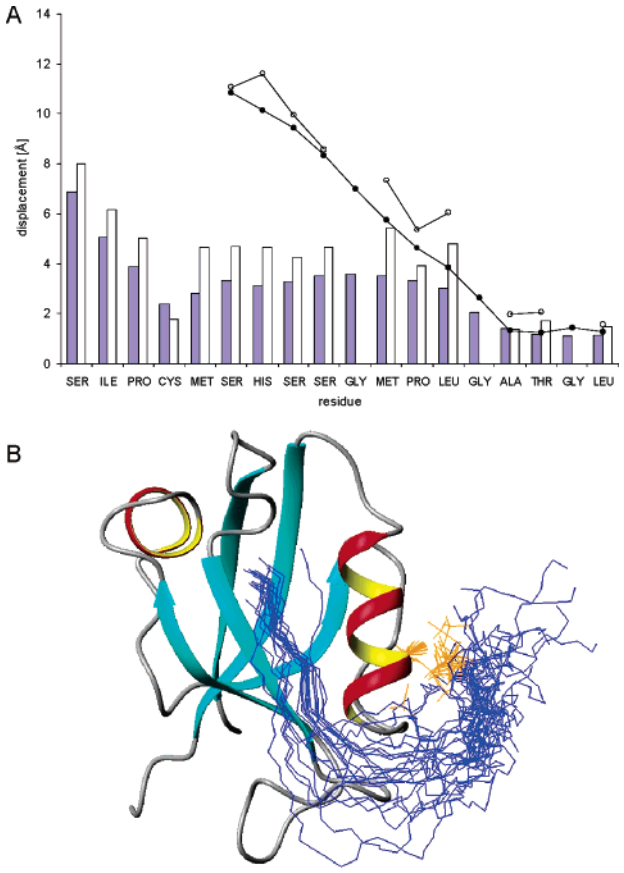

FIGURE 5: (A) Main (shaded) and side chain (empty) displacements of the $GluRA_{13}$ (lines) and $GluRA_{18}$ (bars) peptides in complex with $SAP97_{PDZ2}$ computed from the family of 20 low-energy structures. (B) Ensemble of modeled structures of $SAP97_{PDZ2}$ in complex with $GluRA_{18}$. The PDZ2 main chain is superimposed and shown as a ribbon, and the backbones of the peptide structures are shown with lines. Side chains of the disulfide-forming cysteines are shown specifically.

superimposed on the $SAP97_{PDZ2}$ main chain is modest as expected (Figure 5A, lines). The deviation is small only for the last four C-terminal residues, whereas the rest of the peptide chain is devoid of structure as in that part there were no experimental restraints.

Because of the involvement of a disulfide in the binding of Bio-$GluRA_{18}$ to $SAP97_{PDZ2}$ in the plate binding assay, we continued the NMR experiments by using nonreducing conditions and $GluRA_{18}$ instead of $GluRA_{13}$. Indeed, titrations with $GluRA_{18}$ performed under oxidizing conditions resulted in a change of Cys378 C^{β} resonances from a reduced form resonating at ~28 ppm to an oxidized form at ~41 ppm (*29*), the unambiguous signature of a disulfide-linked complex. The presence of a covalent $GluRA_{18}$−$SAP97_{PDZ2}$ complex was also confirmed by mass spectrometric analysis of the NMR sample, which indicated that within detection limits all $SAP97_{PDZ2}$ molecules are covalently bound to $GluRA_{18}$. The excess of the free GluR-A peptide gradually formed dimers a few days after the initial mixing.

Next, we analyzed whether it is possible for $SAP97_{PDZ2}$ to simultaneously accommodate the C-terminus of $GluRA_{18}$ in its PDZ binding groove and to form a disulfide bond with the Cys residue at the N-terminal part of the peptide. A structural model was built by including a disulfide bond between Cys893 of GluR-A and Cys378 of $SAP97_{PDZ2}$ as well as the restraints used in the previous model. The final

calculation of 100 conformations resulted in a model of a family of 20 low-energy and closely similar GluR-A peptide conformations and side chain rotamers of $SAP97_{PDZ2}$ (Figure 5).

To assess the precision of our model of $GluRA_{18}$, we superimposed the PDZ2 main chain and computed the displacement of the 18-mer peptide just as before for the 13-mer (Figure 5A, columns). The deviation is small for the last four C-terminal residues due to many restraints, and for Cys893 and particularly its side chain, due to the disulfide bridge. Between the cysteine and the C-terminal tetrapeptide, the deviation is larger but evidently limited by the length of the peptide. The three N-terminal residues of $GluRA_{18}$ are widely dispersed in the absence of restraints derived from the NMR spectra. According to our model (Figure 5B), the $GluRA_{18}$ peptide is indeed long enough to reach from the disulfide to the canonical C-terminal binding site and for dispersion to accumulate between them. The model presents a plausible conformation in which the binding is mediated by noncovalent class I interactions involving the C-terminus of GluR-A together with a covalent link between Cys893 of GluR-A and Cys378 of SAP97 (Figure 4B). However, judging from the chemical shift changes of $SAP97_{PDZ2}$ that were detected from the 1:1 covalent complex with $GluRA_{18}$, we found only a minute fraction of the binding pockets are occupied at any instance. This was inferred by comparing the amide chemical shifts of Gly328 (Gly169 in PSD-95) and Ser332 (Ser173 in PSD-95) that experience large secondary shifts with those of the free and fully occupied samples (Figure 6).

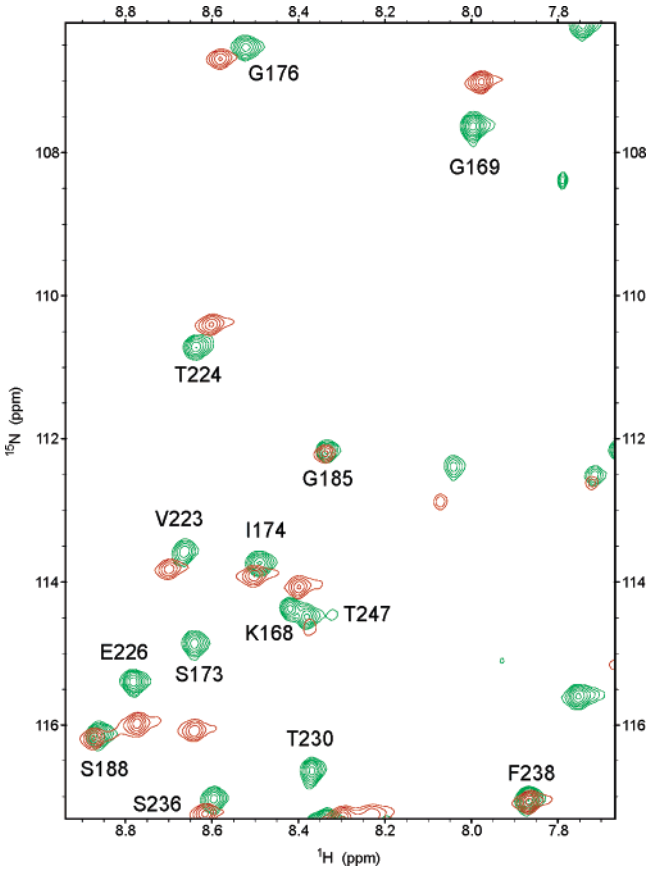

FIGURE 6: Expansions of the overlaid $^{15}N-^{1}H$ correlations from $SAP97_{PDZ2}$ residues Gly169 and Ser173 (numbering refers to PSD-95) free (red) or fully (>95%) occupied (green) by a 10-fold excess of $GluRA_{18}$ peptide. On the other hand, the signals of the 1:1 covalent complex are practically identical to that of the free form and thus imply negligible occupancy of the binding groove.

DISCUSSION

Experimental induction of long-term changes in synaptic strength is often accompanied by selective insertion of GluR-A subunit-containing AMPA receptors into synapses by a mechanism which is dependent on the C-terminal PDZ binding motif of GluR-A. Although the critical PDZ proteins responsible for the interaction have not been identified, the C-terminus of GluR-A binds to PDZ domains of SAP97 (*6*, *10*), and several findings point to a key role for SAP97 in synaptic targeting of GluR-A. SAP97 and GluR-A colocalize in cortical synapses (*30*). SAP97 and GluR-A can be immunoprecipitated as a complex (*6*, *11*, *30*). Overexpression of SAP97 drives GluR-A to synapses in transfected hippocampal neurons (*12*, *13*). RNAi block of SAP97 gene expression inhibits synaptic clustering of GluR-A (*13*). The analysis of the interaction of GluR-A C-terminal peptides with the PDZ2 domain of SAP97 presented here was carried out to gain structural insight into the selectivity, specificity, and regulation of this important interaction.

During the purification, it became evident that $SAP97_{PDZ2}$ has a tendency to form dimers due to the presence of a single reactive cysteine residue at position 378. In the absence of reducing agents, this cysteine together with a cysteine residue in the 18-mer GluR-A peptide (Cys893; position −14, the C-terminal position being designated 0) dominated the interaction, leading to strikingly different binding characteristics depending on redox conditions. Under reducing conditions, a low-affinity PDZ interaction prevailed, whereas in the absence of reducing agents, an intermolecular disulfide bridge stabilized the complex. NMR analysis indicated that in the presence of dithiothreitol, 18- and 13-mer GluR-A peptides bound to $SAP97_{PDZ2}$ in a manner typical for class I PDZ interactions (*4*). The binding was mediated by the most C-terminal tetrapeptide, with essential interactions between residues at positions 0 (C-terminal Leu907) and −2 (Thr905) of the GluR-A peptide and the carboxylate binding GLGF loop, and the side chain of His384 of $SAP97_{PDZ2}$. Apart from a minor contribution of an alanine residue at peptide position −3, no other stabilizing interactions were observed. These results are consistent with our earlier site-directed mutagenesis study showing that individual alanine replacements of residues Thr905 and Leu907 completely eliminated binding of GluR-A CTD to SAP97 PDZ domains in a GST pulldown assay (*10*). Importantly, however, similar peptide chemical shift changes were observed for the titrations with the PDZ2 domains of both SAP97 and PSD-95, yet in the GST pulldown assay, only the former binds to the C-terminal domain of GluR-A (*10*). Furthermore, under reducing conditions, the biotinylated $GluRA_{18}$ peptide did not bind to $SAP97_{PDZ2}$, while a biotinylated and cysteine-free NR2A peptide exhibited specific and avid binding in a microplate binding assay. It is thus obvious that reducing conditions do not reproduce an affinity and specificity expected for a physiological interaction.

Plate binding assays performed in the absence of reducing agents resulted in a different picture. The biotinylated $GluRA_{18}$ peptide displayed covalent binding to $SAP97_{PDZ2}$ which depended on the free thiol in the PDZ domain.

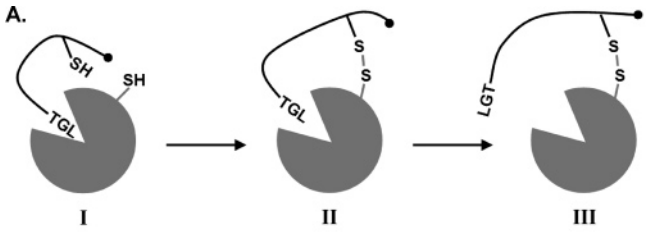

B. GluR-A

HUMAN	VVSHDFPKSMQSIP**C**MSHSSGMPLGATGL
RAT	VVSQDFPKSMQSIP**C**MSHSSGMPLGATGL
CHICKEN	VVSHDFPKSMQTIP**C**MSHSTGMSLGATGL
FROG	VVSHDFPKTMQTIP**C**MSHGAGMSLGATGL
FISH	IVTHDFPKAVQTLP**C**MSHAASMGLGASGM
	DFPK Q PCMSH M LGA G

SAP97

HUMAN	KLQIGDKLLAVNNV**C**LEEVTHEEAVTALK
RAT	KLQIGDKLLAVNSV**C**LEEVTHEEAVTALK
CHICKEN	KLQIGDKLLAVNSV**C**LEEVTHEEAVTALK
FROG	RLQIGDKLLAVNTV**C**LEEVSHEDAVTALK
FISH	RLQIGDKLLAVNSS**C**LEEVTHEHAVTALK
	LQIGDK LAVN CLE V HE AV ALK

FIGURE 7: Role of the disulfide bond in GluR-A−SAP97 interaction. (A) Schematic model of the interaction. (B) Conservation of the critical cysteine residues in GluR-A and SAP97 in major vertebrate classes. Sequence alignment positions the cysteines (bold) and the 14 flanking residues in human, rat, chick, frog, and fish homologues of SAP97 and GluR-A. GenBank/EMBL access codes of the corresponding nucleotide sequence entries are as follows: M81886 for human (*Homo sapiens*), X17184 for rat (*Rattus norvegicus*), X89510 for chicken (*Gallus gallus*), CX504705 for frog (*Xenopus tropicalis*), and AF525741 for zebrafish (*Brachyodanio rerio*).

Although the specificity of the binding of the biotinylated GluR-A peptide to $SAP97_{PDZ2}$ could not be unambiguously determined, due to the covalent nature, negligible binding of Bio-$GluRA_{18}$ to immobilized BSA, containing a single reactive cysteine residue at position 34 (*31*), and relatively little binding to the immobilized N-terminal domain of SAP97, which harbors two cysteine residues (at positions 66 and 73), support a facilitatory contribution of a canonical PDZ interaction to the formation of a covalent adduct.

NMR measurements of $GluRA_{18}$−$SAP97_{PDZ2}$ interaction carried out in the absence of DTT showed an unambiguous sign of the disulfide. Molecular modeling of the $SAP97_{PDZ2}$−$GluRA_{18}$ complex using the NMR data indicated that the cysteine side chain in the $GluRA_{18}$ peptide is able to reach Cys378 of $SAP97_{PDZ2}$, which is situated in a short β-strand on the opposite side of helix B from the PDZ binding groove which houses the C-terminal tetrapeptide of $GluRA_{18}$. However, experiments performed with the covalent $GluRA_{18}$−$SAP97_{PDZ2}$ complex separated from the unbound peptide revealed no sign of PDZ interactions observed under reducing conditions, suggesting that the stabilization of the interaction by disulfide largely excludes binding of the C-terminus to the PDZ binding pocket.

On the basis of the results discussed above, a two-step mechanism for the interaction between SAP97 and the GluR-A C-terminal peptide can be envisioned: an initial low-affinity class I PDZ interaction would bring the reactive thiols of the GluR-A peptide and $SAP97_{PDZ2}$ into proximity (Figure 7A, part I), whereafter, under appropriate redox conditions, an intermolecular disulfide bond would form. After a short-lived state in which both a PDZ interaction and a disulfide bond are present, the complex would convert into a state in which the C-terminus of the peptide is free (Figure 7A, II and III), possibly because of altered conformational dynamics due to the disulfide linkage. This model is consistent with the negligible occupancy of the PDZ binding pocket in the covalent complex and the anomalous peptide binding data. The proposed mechanism is also in good agreement with the strict SAP97 selectivity observed earlier for interaction of GluR-A CTD with the PDZ1−3 domains of four related Maguks in GST pulldown assays (*10*). Only SAP97 has a cysteine residue in the PDZ2 domain, whereas PSD-95 has no cysteine residues in its PDZ domains. In addition, a single cysteine is present in the PDZ1 domains of SAP97, SAP102, and PSD-93. Involvement of disulfide formation in these GST pulldown assays is supported by our finding that the GST fusion of GluR-A CTD and the PDZ2 domain of SAP97 elutes from a glutathione column as a covalent complex under nonreducing conditions (L. von Ossowski and K Keinänen, unpublished observations). In the study mentioned above, an upstream SSG sequence was also found to be important for binding, in addition to the C-terminal PDZ binding motif (*10*). The explanation for this finding is not obvious on the basis of the structural models presented here. The tripeptide sequence is present in the synthetic GluR-A peptides but did not exhibit any specific chemical shift changes upon binding to $SAP97_{PDZ2}$. It is possible that the SSG sequence facilitates the proper flexibility of the C-terminus needed to establish the disulfide bond. Alternatively, the binding specificity of an intact C-terminal domain may be determined by additional mechanisms or even mechanisms different from those observed in the peptide binding studies presented here.

At present, the physiological relevance of disulfide bond formation between $SAP97_{PDZ2}$ and GluR-A is unclear, but it is interesting to note that the responsible cysteine residues in GluR-A and $SAP97_{PDZ2}$ are conserved across major vertebrate phyla from humans to chicken to zebrafish, indicative of a crucial functional or structural importance (Figure 7B). Generally, cytoplasmic redox conditions should not favor formation of disulfide bonds, although cytosolic redox signaling seems to be more widespread than generally appreciated (*32*), and there are examples of cytoplasmic disulfides even in the context of synaptic scaffolding proteins, including disulfide-linked multimers of PSD-95 in the brain (*33*). The disulfide-stabilized complex between a PDZ domain and its target peptide is not without precedent. The N-terminal PDZ domain of InaD, a multidomain scaffolding protein in the fruit fly, forms an intermolecular disulfide bond with a cysteine residue at the −1 position of the C-terminus of its target protein, NorpA (*34*). Quite recently, redox modulation of another PDZ interaction was reported, in this case involving an intramolecular disulfide within the peptide target of PDZ3 of PTP-BL, a phosphotyrosine phosphatase (*35*).

In conclusion, our analysis of the interaction between synthetic C-terminal GluR-A peptides and the PDZ2 domain of SAP97 indicates that the binding mode is strongly dependent on redox conditions. Under reducing conditions, a weak binding determined by typical class I PDZ interactions is observed, whereas in the absence of a reducing agent, an intermolecular disulfide bond is formed. Further studies

are clearly warranted to examine the role of disulfide bonds and redox regulation of native SAP97−GluR-A interaction.

ACKNOWLEDGMENT

We thank Gunilla Rönnholm (Protein Chemistry Unit, Institute of Biotechnology) for technical assistance with mass spectroscopy.

SUPPORTING INFORMATION AVAILABLE

Electrophoretic size of native SAP97 and GluR-A under reducing and nonreducing conditions (Figure 1) and intramolecular nOes observed in $GluRA_{13}$ when in complex with $SAP97_{PDZ2}$ (Table 1). This material is available free of charge via the Internet at http://pubs.acs.org.

REFERENCES

1. Montgomery, J. M., Zamorano, P. L., and Garner, C. C. (2004) MAGUKs in synapse assembly and function: An emerging view, *Cell. Mol. Life Sci. 61*, 911−929.
2. Bredt, D. S., and Nicoll, R. A. (2003) AMPA receptor trafficking at excitatory synapses, *Neuron 40*, 361−379.
3. Malinow, R., and Malenka, R. C. (2002) AMPA receptor trafficking and synaptic plasticity, *Annu. Rev. Neurosci. 25*, 103−126.
4. Hung, A. Y., and Sheng, M. (2002) PDZ domains: Structural modules for protein complex assembly, *J. Biol. Chem. 277*, 5699−5702.
5. Hayashi, Y., Shi, S. H., Esteban, J. A., Piccini, A., Poncer, J. C., and Malinow, R. (2000) Driving AMPA receptors into synapses by LTP and CaMKII: Requirement for GluR1 and PDZ domain interaction, *Science 287*, 2262−2267.
6. Leonard, A. S., Davare, M. A., Horne, M. C., Garner, C. C., and Hell, J. W. (1998) SAP97 is associated with the α-amino-3-hydroxy-5-methylisoxazole-4-propionic acid receptor GluR1 subunit, *J. Biol. Chem. 273*, 19518−19524.
7. Shen, L., Liang, F., Walensky, L. D., and Huganir, R. L. (2000) Regulation of AMPA receptor GluR1 subunit surface expression by a 4.1N-linked actin cytoskeletal association, *J. Neurosci. 20*, 7932−7940.
8. Schulz, T. W., Nakagawa, T., Licznerski, P., Pawlak, V., Kolleker, A., Rozov, A., Kim, J., Dittgen, T., Köhr, G., Sheng, M., Seeburg, P. H., and Osten, P. (2004) Actin/α-actinin-dependent transport of AMPA receptors in dendritic spines: Role of the PDZ-LIM protein RIL, *J. Neurosci. 24*, 8584−8594.
9. Stricker, N. L., and Huganir, R. L. (2003) The PDZ domains of mLin-10 regulate its trans-Golgi network targeting and the surface expression of AMPA receptors, *Neuropharmacology 45*, 837−848.
10. Cai, C., Coleman, S. K., Niemi, K., and Keinänen, K. (2002) Selective binding of synapse-associated protein 97 to GluR-A α-amino-5-hydroxy-3-methyl-4-isoxazole propionate receptor subunit is determined by a novel sequence motif, *J. Biol. Chem. 277*, 31484−31490.
11. Sans, N., Racca, C., Petralia, R. S., Wang, Y. X., McCallum, J., and Wenthold, R. J. (2001) Synapse-associated protein 97 selectively associates with a subset of AMPA receptors early in their biosynthetic pathway, *J. Neurosci. 21*, 7506−7516.
12. Rumbaugh, G., Sia, G. M., Garner, C. C., and Huganir, R. L. (2003) Synapse-associated protein-97 isoform-specific regulation of surface AMPA receptors and synaptic function in cultured neurons, *J. Neurosci. 23*, 4567−4576.
13. Nakagawa, T., Futai, K., Lashuel, H. A., Lo, I., Okamoto, K., Walz, T., Hayashi, Y., and Sheng, M. (2004) Quaternary structure, protein dynamics, and synaptic function of SAP97 controlled by L27 domain interactions, *Neuron 44*, 453−467.
14. Wilkins, M. R., Lindskog, I., Gasteiger, E., Bairoch, A., Sanchez, J.-C., Hochstrasser, D. F., and Appel, R. D. (1997) Detailed peptide characterisation using PEPTIDEMASS: A World-Wide Web accessible tool, *Electrophoresis 18*, 403−408.
15. Sattler, M., Schleucher, J., and Griesinger, C. (1999) Heteronuclear multidimensional NMR experiments for the structure determination of proteins in solution employing pulsed field gradients, *Prog. NMR Spectrosc. 34*, 93−158.
16. Permi, P., and Annila, A. (2004) Coherence transfer in proteins, *Prog. NMR Spectrosc. 44*, 97−137.
17. Permi, P., Tossavainen, H., and Hellman, M. (2004) Efficient assignment of methyl resonances: enhanced sensitivity by gradient selection in a DE-MQ-(H)CC*m*H*m*-TOCSY experiment, *J. Biomol. NMR 30*, 275−282.
18. Zimmerman, D. E., Kulikowski, C. A., Huang, Y., Feng, W., Tashiro, M., Shimotakahara, S., Chien, C., Powers, R., and Montelione, G. T. (1997) Automated analysis of protein NMR assignments using methods from artificial intelligence, *J. Mol. Biol. 269*, 592−610.
19. Wüthrich, K. (1986) *NMR of proteins and nucleic acids*, John Wiley & Sons, New York.
20. Grzesiek, S., Bax, A., Clore, G. M., Gronenborn, A. M., Hu, J. S., Kaufman, J., Palmer, I., Stahl, S. J., and Wingfield, P. T. (1996) The solution structure of HIV-1 Nef reveals an unexpected fold and permits delineation of the binding surface for the SH3 domain of Hck tyrosine protein kinase, *Nat. Struct. Biol. 3*, 340−345.
21. Nilges, M. (1995) Calculation of protein structures with ambiguous distance restraints. Automated assignment of ambiguous NOE crosspeaks and disulfide connectivities, *J. Mol. Biol. 245*, 645−660.
22. Kuszewski, J., Gronenborn, A. M., and Clore, G. M. (1996) Improving the quality of NMR and crystallographic protein structures by means of a conformational database potential derived from structure databases, *Protein Sci. 5*, 1067−1080.
23. Niethammer, M., Kim, E., and Sheng, M. (1996) Interaction between the C terminus of NMDA receptor subunits and multiple members of the PSD-95 family of membrane-associated guanylate kinases, *J. Neurosci. 16*, 2157−2163.
24. Lim, I. A., Hall, D. D., and Hell, J. W. (2002) Selectivity and promiscuity of the first and second PDZ domains of PSD-95 and synapse-associated protein 102, *J. Biol. Chem. 277*, 21697−21711.
25. Lim, I. A., Merrill, M. A., Chen, Y., and Hell, J. W. (2003) Disruption of the NMDA receptor-PSD-95 interaction in hippocampal neurons with no obvious physiological short-term effect, *Neuropharmacology 45*, 738−754.
26. Tochio, H., Hung, F., Li, M., Bredt, D. S., and Zhang, M. (2000) Solution structure and backbone dynamics of the second PDZ domain of postsynaptic density-95, *J. Mol. Biol. 295*, 225−237.
27. Wang, P., Zhang, Q., Tochio, H., Fan, J. S., and Zhang, M. (2000) Formation of a native-like β-hairpin finger structure of a peptide from the extended PDZ domain of neuronal nitric oxide synthase in aqueous solution, *Eur. J. Biochem. 267*, 3116−3122.
28. Clore, G. M., and Schwieters, C. D. (2003) Docking of protein−protein complexes on the basis of highly ambiguous intermolecular distance restraints derived from $^{1}H/^{15}N$ chemical shift mapping and backbone ^{15}N-^{1}H residual dipolar couplings using conjoined rigid body/torsion angle dynamics, *J. Am. Chem. Soc. 125*, 2902−2912.
29. Cavanagh, J., Fairbrother, W., Palmer, A., and Skelton, N. (1995) *Protein NMR Spectroscopy: Principles and Practices*, Academic Press, San Diego.
30. Valtschanoff, J. G., Buret, A., Davare, M. A., Leonard, A. S., Hell, J. W., and Weinberg, R. J. (2000) SAP97 concentrates at the postsynaptic density in cerebral cortex, *Eur. J. Neurosci. 12*, 3605−3614.
31. Kuwata, K., Era, S., and Sogami, M. (1994) The kinetic studies on the intramolecular SH, S-S exchange reaction of bovine mercaptalbumin, *Biochim. Biophys. Acta 1205*, 317−324.
32. Leichert, L. I., and Jakob, U. (2004) Protein thiol modifications visualized in vivo, *PLoS Biol. 2*, 1723−1737.
33. Hsueh, Y. P., Kim, E., and Sheng, M. (1997) Disulfide-linked head-to-head multimerization in the mechanism of ion channel clustering by PSD-95, *Neuron 18*, 803−814.
34. Kimple, M. E., Siderovski, D. P., and Sondek, J. (2001) Functional relevance of the disulfide-linked complex of the N-terminal PDZ domain of InaD with NorpA, *EMBO J. 20*, 4414−4422.
35. van den Berk, L. C. J., Landi, E., Harmsen, E., Dente, L., and Hendriks, W. J. A. J. (2005) Redox-regulated affinity of the third PDZ domain in phosphotyrosine phosphatase PTP-BL for cysteine-containing target peptides, *FEBS Lett. 272*, 3306−3316.

BI0511989